JOURNAL OF MATERIALS SCIENCE 19 (1984) 4138–4146

Linearized equations for the electronic transport properties of thin metal films

V. I. VATAMANYUK*, A. J. TOSSER, C. R. PICHARD
Laboratoire d'Electronique, Universite de Nancy, 1, B.P. 239, 54506 Vandoeuvre-les-Nancy, France

C. R. TELLIER
Laboratoire de Chronometrie et Piezoelectricite, ENSMM, La Bouloie, Route de Gray, 25030 Besancon, France

Starting from the multidimensional statistical model of grain boundaries a new unique general expression is proposed for the resistivity, the temperature coefficient of resistivity and the Hall coefficient of monocrystalline, polycrstalline and columnar films. The ranges of validity of linearized equations are determined. Experiments of other workers related to columnar films are interpreted satisfactorily in this way.

1. Introduction

Many types of scattering could exist in a thin metal film; however, in this paper related to size effects, we only consider the three following sources of scattering:

1. The background scattering whose effect is usually represented by the mean free path of the electron in the bulk material, λ_0 [1, 2];

2. The scattering at the external surfaces of the metal film, due to the mechanical roughness of the surface; this phenomenon is the origin for the usual Fuchs–Sondheimer size effect [2];

3. The scattering at grain boundaries. Its effect on transport properties may be represented either by parameters derived from quantum mechanical calculations [3] or by statistical parameters introduced for a physical description of the phenomenon [4]. It has been pointed out [3, 4] that the electrical resistivity calculated in the Mayadas–Shatzkes model (M.–S. model) [3], reduces to the bulk resistivity when the grain boundaries are distributed regularly in the film, whereas it is not the case for the statistical models [4]; moreover, the M.–S. model does not allow the calculation of the Hall coefficients [5] since it is a unidimensional representation of multidimensional phenomena, as previously emphasized in several remarks [4, 6]. It is the reason why we restrict our attention to the models based on statistical parameters [6–10]; the models proposed by Warkusz [11] are not retained because the validity of some mathematical equations seems doubtful [4, 12, 13], even if the derived approximate equations do not markedly deviate from the true ones in some limiting cases [14]. Therefore, the scattering at external surfaces is represented by a mean free path, λ_s, initially proposed by Cottey [15] and the grain-boundary scattering is represented by a mean free path, λ_g, calculated in the framework of a three-dimensional [4, 16] or bidimensional [8] grain-boundary model.

The total mean free path, λ, is then written, as usual [4] as:

$$\lambda^{-1} = \lambda_0^{-1} + \lambda_s^{-1} + \lambda_g^{-1} \quad (1)$$

Under these assumptions, the calculations of the electrical resistivity and its temperature coefficient and the Hall coefficient are made in the case of films exhibiting a polycrystalline [17], monocrystalline [17], and columnar structure [18].

A comparison between the approximate and exact equations is the aim of this paper.

*Permanent address: Physics Institute Ukrainian Academy of Sciences, 144pr. Nauki, Kiev 28, URSS.

0022–2461/84 $03.00 + .12

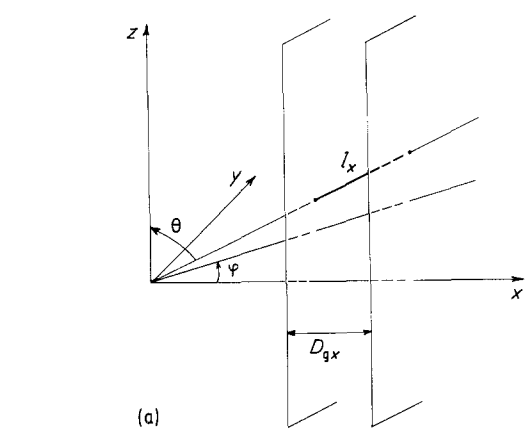

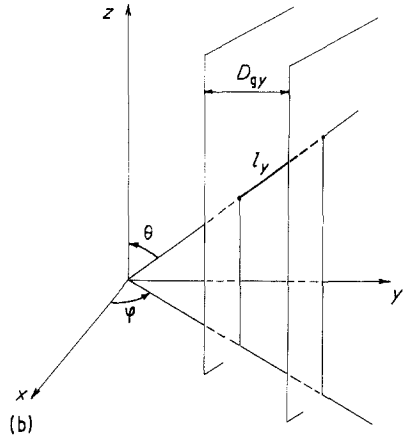

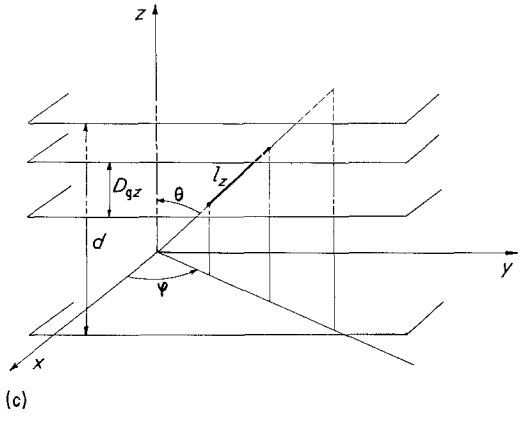

Figure 1 (a) The array of planar scatterers perpendicular to the x-axis. (b) The array of planar scatterers perpendicular to the y-axis. (c) The array of planar scatterers perpendicular to the z-axis.

2. Theoretical equations

2.1. Electrical conductivity

If the grain boundaries perpendicular to the x-axis (y-, z-) are represented by a regular array of planar scatterers, with spacing D_{gx} (D_{gy}, D_{gz}), (Fig. 1) and if the statistical electron transmission coefficient, t, describes the effect of any grain boundary on the electron flow crossing any grain boundary, the electronic mean free path λ_x (λ_y, λ_z) describing the scattering is given by [4, 16]:

$$\lambda_x^{-1} = D_{gx}^{-1} \ln \frac{1}{t} |\cos \phi| \, |\sin \theta| \tag{2}$$

$$\lambda_y^{-1} = D_{gy}^{-1} \ln \frac{1}{t} |\sin \phi| \, |\sin \theta| \tag{3}$$

$$\lambda_z^{-1} = D_{gz}^{-1} \ln \frac{1}{t} |\cos \theta| \tag{4}$$

In the framework of the extension [19] of the Cottey model [15] the electronic scattering at external surfaces is represented by a mean free path, λ_s, given by [4, 19]:

$$\lambda_s^{-1} = d^{-1} \ln \frac{1}{p} |\cos \theta| \tag{5}$$

where p is the usual specular reflection coefficient, initially introduced by Fuchs [1] and d is the film thickness.

When the grain boundaries are distributed in three dimensions the resultant mean free path, λ, derived from Equation 1, is expressed by:

$$\lambda(\theta)^{-1} = \lambda_0^{-1} \left[1 + \frac{C^2}{\nu} + |\cos \theta| \left(\frac{1 - C}{\nu} + \frac{1}{\mu} \right) \right] \tag{6}$$

assuming that:

$$D_{gx} = D_{gy} = D_{gz} = D_g \tag{7}$$

$$|\cos \phi| + |\sin \phi| = C = 4/\pi \tag{8}$$

with:

$$\nu = D_g \lambda_0^{-1} \left(\ln \frac{1}{t} \right)^{-1} \tag{9}$$

$$\mu = d \lambda_0^{-1} \left(\ln \frac{1}{p} \right)^{-1} \tag{10}$$

When there is no grain boundary parallel to the film surface, the resultant mean free path, λ, is expressed as [4, 8]:

$$\lambda(\theta)^{-1} = \lambda_0^{-1} \left[1 + \frac{C^2}{\nu} + |\cos \theta| \left(-\frac{C}{\nu} + \frac{1}{\mu} \right) \right] \tag{11}$$

assuming that:

$$D_{gx} = D_{gy} = D_g \tag{12}$$

$$|\cos \phi| + |\sin \phi| = C \tag{13}$$

ν and μ having the same definition as above.

Following the usual method for calculating the conductivity, σ_f, [4] yields, respectively:

$$\sigma_{fi} = \sigma_0 \frac{3}{2b_i}\{a_i - \tfrac{1}{2} + (1 - a_i^2)\ln(1 + a_i^{-1})\} \quad (14)$$

with $i = 2, 3$

$$a_2 = (1 + C^2\nu^{-1})b_2^{-1} \quad (15)$$

$$a_3 = (1 + C^2\nu^{-1})b_3^{-1} \quad (16)$$

$$b_2 = \mu^{-1} - C\nu^{-1} \quad (17)$$

$$b_3 = \mu^{-1} + (1 - C)\nu^{-1} \quad (18)$$

σ_0 being the bulk conductivity and μ and ν being defined by Equations 10 and 9, respectively.

Assuming that D_g does not vary with thickness, and takes values lower than the film thickness, Equation 14 (for $i = 3$) expresses the conductivity of polycrystalline films, as previously shown [4, 16]. Assuming that:

$$D_g = d \quad (19)$$

Equation 14 (for $i = 2$) expresses the conductivity of monocrystalline films, in agreement with previous results [4, 8].

In the case where D_g is not thickness dependent, Equation 14 can express the conductivity of a thin film grown in a columnar fashion, as recently shown [9].

In the limiting case where the effect of grain boundaries vanishes, i.e. for $D_g \to \infty$, $\nu \to \infty$, therefore:

$$b_i \to \mu^{-1}; \quad a_i \to b_i^{-1}$$

and:

$$\left.\frac{\sigma_{fi}}{\sigma_0}\right|_{D_g \to \infty} \longrightarrow \frac{3a}{2}\{a - \tfrac{1}{2} + (1 - a^2)\ln(1 + a^{-1})\} = \mathscr{C}(a) \quad (20)$$

which is the Cottey function, $\mathscr{C}(a)$, [15], as attempted.

2.2. Temperature coefficient of resistivity

Neglecting any thermal variation in geometrical and electrical parameters, except in the bulk mean free path, λ_0, the general expression of the temperature coefficient of resistivity (tcr), β_f, is given by [4, 20]:

$$\beta_f = -\frac{\mathrm{d}\ln\sigma_f}{\mathrm{d}T} \quad (21)$$

where T is the absolute temperature, and can be calculated from the following relationship:

$$\beta_f = -\frac{\partial \ln \sigma_f}{\partial \ln \lambda_0}\frac{\partial \ln \lambda_0}{\partial T} \quad (22)$$

Introducing the bulk tcr, β_0, defined by:

$$\frac{\partial \ln \lambda_0}{\partial T} = -\beta_0 \quad (23)$$

Equation 22 takes the form:

$$\frac{\beta_f}{\beta_0} = \frac{\partial \ln \sigma_f}{\partial \ln \lambda_0} \quad (24)$$

We thus obtain, from Equations 14 and 15:

$$\frac{\beta_{fi}}{\beta_0} = \frac{1}{b_i}[a_i^{-1} - 2 + 2a_i \ln(1 + a_i^{-1})] \times [a_i - \tfrac{1}{2} + (1 - a_i^2)\ln(1 + a_i^{-1})]^{-1} \quad (25)$$

with $i = 2, 3$.

For $D_g = d$ and $i = 2$, Equation 25 agrees with the previously published expression for monocrystalline-film tcr [4, 8]; for D_g = constant ($D_g < d$) and $i = 3$, Equation 25 agrees with the expression of polycrystalline-film tcr [4, 21]; for D_g = constant and $i = 2$, Equation 25 gives the expression for the tcr of columnar films.

2.3. The Hall coefficient

It has been recently established [4, 22] that the Hall coefficient at low magnetic field, R_{Hfi}, can be expressed in the form:

$$R_{Hfi}/R_{H\infty} = \beta_{fi}\rho_{fi}/\beta_\infty\rho_\infty \quad (26)$$

where $R_{H\infty}$ is the Hall coefficient of an infinitely thick film, having the same structure as the film, and where the index ∞ is related to the infinitely thick film.

In the absence of impurities, it has been shown [4, 23] that:

$$R_{H\infty} = R_{H0} \quad (27)$$

$$\beta_\infty\rho_\infty = \beta_0\rho_0 \quad (28)$$

where the index 0 is related to the bulk material.

One must not overlook the fact that Equations 27 and 28 are valid even if scatterings at grain boundaries are operative in the infinitely thick film, i.e. for polycrystalline or columnar films especially.

Therefore, in the absence of impurities, Equation 26 takes the following form:

$$R_{Hfi}/R_{H0} = \beta_{fi}\rho_{fi}/\beta_0\rho_0 \quad (29)$$

with $i = 2, 3$.

As in the above paragraphs, the case of monocrystalline, polycrystalline and columnar films correspond to $i = 2$ and $D_g = d$, $i = 3$ and $D_g =$

constant $< d$, $i = 2$ and D_g = constant $\gtrsim d$, respectively.

The explicit analytical expression for the reduced Hall coefficient, R_{Hfi}/R_{H0}, is easily derived from Equations 29, 25 and 14:

$$\frac{R_{Hfi}}{R_{H0}} = \frac{2}{3}\frac{a_i^{-1} - 2 + 2a_i \ln(1 + a_i^{-1})}{[a_i - \frac{1}{2} + (1 - a_i^2)\ln(1 + a_i^{-1})]^2} \tag{30}$$

This result agrees with a direct calculation [17, 22] obtained from the Sondheimer calculation procedure [17, 24].

For the limiting case where the effects of grain boundaries vanishes, i.e. for $D_g \to \infty$, a_i reduces to the generalized Cottey parameter [4, 19] μ and Equation 30 is identical to an expression [17, 25] derived in the framework of the Fuchs–Sondheimer conduction model [2].

3. Approximate equations at large thicknesses

3.1. General remarks

Since there is a formal analogy between Equation 30 and the theoretical expression obtained [25] in the framework of the Cottey model [15] the asymptotical forms for Equations 14, 25 and 30 can be directly derived from the following limiting forms, previously obtained [15, 26] in the framework of the Cottey model.

$$\tfrac{3}{2}a_i[a_i - \tfrac{1}{2} + (1 - a_i^2)\ln(1 + a_i^{-1})] \approx 1 - \frac{3}{8a_i} + \frac{1}{5a_i^2}; \quad |a_i| \to \infty \tag{31}$$

$$\tfrac{3}{2}a_i[1 - 2a_i + 2a_i^2 \ln(1 + a_i^{-1})] \approx 1 - \frac{3}{4a_i} + \frac{3}{5a_i^2}; \quad a_i \to \infty \tag{32}$$

At this step of the linearization procedure we do not examine whether the condition $|a_i| \to \infty$ corresponds to an asymptotic value for d (and D_g), we only want to compare the linearized equations with exact equations.

3.2. The linearized forms for Equations 14, 25 and 30

From Equations 31 and 32 the following linearized equations are derived (using Equations 14, 25 and 30):

$$\frac{\sigma_f}{\sigma_0} \approx \frac{1}{a_i b_i}\left(1 - \frac{3}{8a_i}\right) \tag{33}$$

$$\frac{\beta_f}{\beta_0} \approx \frac{1}{a_i b_i}\left(1 - \frac{3}{8a_i}\right) \tag{34}$$

$$\frac{R_{Hf}}{R_{H0}} \approx \left[1 + \left(\frac{1}{5} - \frac{9}{64}\right)\frac{1}{a_i^2}\right] \tag{35}$$

Alternative forms for these equations could be:

$$\frac{\rho_f}{\rho_0} \approx a_i b_i \left(1 + \frac{3}{8a_i}\right) \tag{36}$$

$$\frac{\beta_0}{\beta_f} \approx a_i b_i \left(1 + \frac{3}{8a_i}\right) \tag{37}$$

$$\frac{R_{H0}}{R_{Hf}} \approx \left[1 - \left(\frac{1}{5} - \frac{9}{64}\right)\frac{1}{a_i^2}\right] \tag{38}$$

A deviation from the exact equations of less than 5% is obtained with the linearized Equations 33, 34, 36 and 37, provided that the condition:

$$|a_i| \geqslant 2 \tag{39}$$

and:

$$a_i \geqslant 1; \quad a_i \leqslant -2 \tag{40}$$

are satisfied, respectively, whatever the value of b_i.

A deviation from the exact equation of less than 5% is obtained with the linearized Equation 35 provided that $a_i \geqslant 0.8$ or $a_i < 0$. The linearized Equation 38 is less accurate.

With the aid of Equations 12 and 18 the above conditions can be interpreted in the framework of the multidimensional models to give the ranges of validity of the linearized Equations 33, 34 and 35 in the case of polycrystalline, monocrystalline and columnar structures (Table I). The same analysis can be made with Equations 36 to 38 (Table II).

It can be concluded that the best set of linearized equations for monocrystalline, polycrystalline and columnar structures are Equations 36 to 38.

From Tables I and II it may be concluded that the range of validity of Equations 36 to 38 is larger than that of Equations 33 to 35.

3.3. The special case where grain boundaries are operative at infinite thickness

In the case of infinitely thick polycrystalline or columnar films, the parameters a_i and b_i are replaced by:

$$a_{3\infty} = (1 + C^2\nu^{-1})b_{3\infty}^{-1} \tag{41}$$

$$b_{3\infty} = (1 - C)\nu^{-1} \tag{42}$$

and:

$$|a_{2\infty}| = (1 + C^2\nu^{-1})b_{2\infty}^{-1} \tag{43}$$

$$b_{2\infty} = -C\nu^{-1} \tag{44}$$

TABLE I Ranges of validity of the linearized Equations 33 to 35 for polycrystalline (Pol.), monocrystalline (Mono.) and columnar (Col.) films

Row*		$\frac{D_g}{\lambda_0}$	P							
			0.2	0.3	0.4	0.5	0.6	0.7	0.8	0.9
	$t = 0.3$									
1 ($\times 10^{-4}$)		0.001	12.3	9.2	7.01	5.3	3.91	2.73	1.71	0.81
2 ($\times 10^{-3}$)	Pol.	0.01	12.3	9.2	6.99	5.29	3.89	2.72	1.7	0.8
3 ($\times 10^{-2}$)	$\frac{d}{\lambda_0} \geqslant$	0.1	11.9	8.88	6.75	5.11	3.77	2.63	1.65	0.78
4 ($\times 10^{-1}$)		0.5	5.23	3.92	2.98	2.25	1.66	1.16	0.73	0.34
5 ($\times 10^{-4}$)		0.001	6.41 / 28.9	4.8 / 21.6	3.65 / 16.4	2.76 / 12.3	2.03 / 9.2	1.42 / 6.4	0.89 / 4.0	0.42 / 1.9
6 ($\times 10^{-3}$)	Col.	0.01	6.4 / 29.1	4.8 / 21.8	3.65 / 16.6	2.76 / 12.5	2.03 / 9.2	1.42 / 6.5	0.89 / 4.0	0.42 / 1.9
7 ($\times 10^{-2}$)	$\frac{d}{\lambda_0} \geqslant \leqslant$	0.1	6.29 / 32.0	4.7 / 23.0	3.58 / 18.0	2.71 / 14.0	2.0 / 10.0	1.39 / 7.0	0.87 / 4.3	0.41 / 2.1
8 ($\times 10^{-1}$)		0.5	2.92 / 26.2	2.18 / 12.1	1.66 / 9.2	1.26 / 7.0	0.93 / 5.1	0.65 / 3.6	0.4 / 2.2	0.19 / 1.7
9 ($\times 10^{0}$)	Mono. $\frac{d}{\lambda_0} \geqslant$	$D_g = d$	0	0	0	0	0.09	0.4	0.67	0.9
	$t = 0.6$									
10 ($\times 10^{-4}$)		0.001	29	21.7	16.5	12.5	9.2	6.43	4.02	1.9
11 ($\times 10^{-3}$)	Pol.	0.01	28.7	21.5	16.4	12.4	9.13	6.37	3.98	1.88
12 ($\times 10^{-2}$)	$\frac{d}{\lambda_0} \geqslant$	0.1	26.6	19.9	15.2	11.5	8.45	5.9	3.69	1.74
13 ($\times 10^{-1}$)		0.5	9.99	7.48	5.69	11.31	3.17	2.21	1.39	0.65
14 ($\times 10^{-4}$)		0.001	15.1 / 68.2	11.3 / 51.0	8.6 / 38.8	6.5 / 29.4	4.8 / 21.6	3.35 / 15.1	2.1 / 9.4	0.99 / 4.5
15 ($\times 10^{-3}$)	Col.	0.01	15.1 / 69.5	11.3 / 52.0	8.6 / 40.0	6.5 / 29.9	4.8 / 22.0	3.35 / 15.4	2.1 / 9.6	0.98 / 4.5
16 ($\times 10^{-2}$)	$\frac{d}{\lambda_0} \geqslant \leqslant$	0.1	14.4 / 86.0	10.8 / 64.0	8.22 / 49.0	6.22 / 37.0	4.58 / 27.0	3.2 / 19.0	2.0 / 11.0	0.95 / 5.6
17 ($\times 10^{-1}$)	$\frac{d}{\lambda_0} \geqslant$	0.5	6.12	4.58	3.48	2.64	1.94	1.37	0.85	0.4
18 ($\times 10^{0}$)	Mono. $\frac{d}{\lambda_0} \geqslant$	$D_g = d$	1.09	0.28	0	0	0	0	0.027	0.26
	$t = 0.9$									
19 ($\times 10^{-3}$)		0.001	14.1	10.5	8.0	6.51	4.46	3.12	1.95	0.92
20 ($\times 10^{-2}$)	Pol.	0.01	13.5	10.1	7.7	5.82	4.29	3.0	1.88	0.89
21 ($\times 10^{-1}$)	$\frac{d}{\lambda_0} \geqslant$	0.1	9.8	7.34	5.6	4.23	3.11	2.17	1.36	0.64
22 ($\times 10^{0}$)		0.5	2.21	1.65	1.26	0.95	0.7	0.49	0.31	0.15
23 ($\times 10^{-3}$)		0.001	7.31 / 33.3	5.47 / 24.9	4.16 / 19.0	3.15 / 14.3	2.32 / 10.6	1.62 / 7.4	1.01 / 4.6	0.48 / 2.2
24 ($\times 10^{-2}$)	Col.	0.01	7.17 / 37.0	5.36 / 27.0	4.08 / 20.0	3.1 / 16.0	2.28 / 11.0	1.6 / 8.0	0.94 / 5.0	0.47 / 2.4
25 ($\times 10^{-1}$)	$\frac{d}{\lambda_0} \geqslant \leqslant$	0.1	5.97	4.47	3.4	2.57	1.9	1.32	0.83	0.39
26 ($\times 10^{0}$)	$\frac{d}{\lambda_0} \geqslant$	0.5	1.72	1.28	0.98	0.74	0.54	0.38	0.24	0.11
27 ($\times 10^{0}$)	Mono. $\frac{d}{\lambda_0} \geqslant$	$D_g = d$	2.78	1.97	1.39	0.95	0.58	0.27	0.007	0

*Each entry in rows 3–10 is multiplied by the appropriate factor in parentheses in column 1.

TABLE II Ranges of validity of the linearized Equations 36 to 38 for polycrystalline (Pol.), monocrystalline (Mono.) and columnar (Col.) films

Row*		$\frac{D_g}{\lambda_0}$	P							
			0.2	0.3	0.4	0.5	0.6	0.7	0.8	0.9
1 (× 10^{-4})	$t = 0.3$									
		0.001	7.05	5.27	4.01	3.04	2.24	1.56	0.97	0.46
2 (× 10^{-3})	Pol.	0.01	7.02	5.25	4.0	3.02	2.23	1.56	0.97	0.46
3 (× 10^{-2})	$\frac{d}{\lambda_0} \geqslant$	0.1	6.76	5.05	3.85	2.9	2.14	1.5	0.93	0.44
4 (× 10^{-1})		0.5	2.89	2.2	1.6	1.25	0.92	0.64	0.4	0.19
5 (× 10^{-4})		0.001	4.61 / 28.9	3.5 / 21.6	2.66 / 16.4	1.98 / 12.3	1.48 / 9.2	1.04 / 6.4	0.65 / 4.0	0.3 / 1.9
6 (× 10^{-3})	Col.	0.01	4.6 / 29.1	3.44 / 21.8	2.62 / 16.6	1.98 / 12.5	1.46 / 9.2	1.02 / 6.5	0.64 / 4.0	0.3 / 1.9
7 (× 10^{-2})	$\frac{d}{\lambda_0} \geqslant \leqslant$	0.1	4.48 / 32.0	3.35 / 23.0	2.55 / 18.0	1.93 / 14.0	1.42 / 11.0	0.99 / 7.0	0.62 / 4.3	0.29 / 2.1
8 (× 10^{-1})		0.5	2.0 / 26.2	1.5 / 12.1	1.1 / 9.2	0.87 / 7.0	0.64 / 5.1	0.45 / 3.6	0.28 / 2.2	0.13 / 1.7
9 (× 10^{0})	Mono. $\frac{d}{\lambda_0} \geqslant$	$D_g = d$	0	0	0	0	0.09	0.4	0.67	0.9
	$t = 0.6$									
10 (× 10^{-4})		0.001	16.6	12.4	9.4	7.15	5.27	3.68	2.3	1.09
11 (× 10^{-3})	Pol.	0.01	16.5	12.3	9.37	7.09	5.22	3.65	2.28	1.08
12 (× 10^{-2})	$\frac{d}{\lambda_0} \geqslant$	0.1	15.0	11.0	8.6	6.5	4.78	3.34	2.09	0.98
13 (× 10^{-1})		0.5	5.49	4.1	3.1	2.36	1.7	1.2	0.76	0.36
14 (× 10^{-4})		0.001	10.9 / 68.2	8.12 / 51.0	6.18 / 38.8	4.68 / 29.4	3.44 / 21.6	2.41 / 15.1	1.5 / 9.4	0.71 / 4.5
15 (× 10^{-3})	Col.	0.01	10.8 / 69.5	8.07 / 52.0	6.15 / 40.0	4.65 / 29.9	3.43 / 22.0	2.39 / 15.4	1.5 / 9.6	0.71 / 4.5
16 (× 10^{-2})	$\frac{d}{\lambda_0} \geqslant \leqslant$	0.1	10.0 / 86.0	7.62 / 64.0	5.8 / 49.0	4.38 / 37.0	3.23 / 27.0	2.26 / 19.0	1.41 / 11.0	0.67 / 5.6
17 (× 10^{-1})	$\frac{d}{\lambda_0} \geqslant$	0.5	4.0	3.0	2.3	1.75	1.3	0.9	0.56	0.27
18 (× 10^{0})	Mono. $\frac{d}{\lambda_0} \geqslant$	$D_g = d$	0.13	0	0	0	0	0	0.027	0.26
	$t = 0.9$									
19 (× 10^{3})		0.001	8.02	6.0	4.57	3.45	2.55	1.78	1.11	0.53
20 (× 10^{-2})	Pol.	0.01	7.68	5.74	4.37	3.3	2.44	1.7	1.06	0.5
21 (× 10^{-1})	$\frac{d}{\lambda_0} \geqslant$	0.1	5.4	4.0	3.1	2.3	1.7	1.2	0.74	0.35
22 (× 10^{0})		0.5	11.5	8.6	6.5	4.95	3.7	2.5	1.6	0.75
23 (× 10^{-3})		0.001	5.25 / 33.3	3.93 / 24.9	3.0 / 19.0	2.26 / 14.5	1.67 / 10.6	1.16 / 7.4	0.73 / 4.6	0.34 / 2.2
24 (× 10^{-2})	Col.	0.01	5.1 / 37.0	3.82 / 27.0	2.9 / 20.0	2.2 / 16.0	1.62 / 11.0	1.13 / 8.0	0.71 / 5.0	0.33 / 2.4
25 (× 10^{-1})	$\frac{d}{\lambda_0} \geqslant \leqslant$	0.1	4.0	3.0	2.3	1.7	1.3	0.88	0.55	0.26
26 (× 10^{-1})	$\frac{d}{\lambda_0} \geqslant$	0.5	9.99	7.5	5.7	4.3	3.2	2.2	1.4	0.65
27 (× 10^{0})	Mono. $\frac{d}{\lambda_0} \geqslant$	$D_g = d$	1.3	0.9	0.61	0.39	0.21	0.05	0	0

*Each entry in rows 3–10 is multiplied by the appropriate factor in parentheses in column 1.

It is easily seen that:

$$a_{3\infty} = -\frac{\nu + C^2}{C-1} < 0$$

with

$$|a_{3\infty}| = \frac{\nu}{C-1} + \frac{C^2}{C-1} > \frac{C^2}{C-1} = 5.92 \quad (45)$$

and:

$$a_{2\infty} = -\frac{\nu + C^2}{C} < 0$$

with

$$|a_{2\infty}| = \frac{\nu}{C} + C > C = 1.27 \quad (46)$$

Introducing $a_{2\infty}$ and $b_{2\infty}$ or $a_{3\infty}$ and $b_{3\infty}$ into the linearized Equations 33 to 38 give the expressions for the approximate reduced parameters related to infinitely thick columnar film (marked by index c) and infinitely thick polycrystalline film (marked by index g), respectively [27].

Due to the value of $|a_{3\infty}|$ the linearized Equations 33 to 38 for σ_g/σ_0, β_0/β_g, R_{Hg}/R_{H0}, ρ_g/ρ_0, β_g/β_0, R_{H0}/R_{Hg} are valid for $a_{3\infty}$ and $b_{3\infty}$ without any restriction since Equation 41 is satisfied.

Due to the value of $|a_{2\infty}|$ the lineared Equations 33 to 38 for σ_c/σ_0, β_0/β_c, R_{Hc}/R_{H0}, ρ_c/ρ_0, β_c/β_0, R_{H0}/R_{Hc} are valid for $a_{2\infty}$ and $b_{2\infty}$, provided that ν takes values greater than 0.93.

From Equations 45, 46, 35 and 38, it is easily seen that R_{Hg} and R_{Hc} practically reduced to R_{H0}, in good agreement with previous direct calculations [28, 29].

3.4. Linearized reduced equations for polycrystalline films

The linearized Equations 33 to 38 may be used for both a film of a given thickness and infinitely thick polycrystalline or columnar films. Several expressions can thus be obtained for the reduced film parameters (with respect to the infinitely thick film).

For any given reduced parameter, the set of the approximate expressions is large and the most accurate expression must be empirically found. For instance, in the case of ρ_f/ρ_g, one can successively write the following equations.

Equation 36 gives:

$$\frac{\rho_f}{\rho_g} \approx \left(1 + \frac{3}{8a_3}\right)\left(1 + \frac{3}{8a_{3\infty}}\right)^{-1} \quad (47)$$

whose two alternative forms are:

$$\frac{\rho_f}{\rho_g} \approx 1 + \frac{3}{8}\frac{a_3^{-1} - a_{3\infty}^{-1}}{1 + (3/8)a_{3\infty}^{-1}}$$

$$= 1 + \frac{3}{8\mu}\frac{1}{1 + [C^2 + (3/8)(1-C)](1/\nu)} \quad (48)$$

and:

$$\frac{\rho_f}{\rho_g} \approx 1 + (3/8)(a_3^{-1} - a_{3\infty}^{-1})$$

$$= 1 + \frac{3}{8\mu}\frac{1}{1 + (C^2/\nu)}; \quad \frac{3}{8a_{3\infty}} \ll 1 \quad (49)$$

Similarly, from Equation 33 we derive:

$$\frac{\rho_f}{\rho_g} \approx 1 + \frac{3}{8}\frac{a_3^{-1} - a_{3\infty}^{-1}}{1 - (3/8)a_{3\infty}^{-1}}$$

$$= 1 + \frac{3}{8\mu}\frac{1}{1 + [C^2 - (3/8)(1-C)](1/\nu)} \quad (50)$$

From the tabulated numerical values [16] it is seen that Equation 50 is the more accurate, moreover the range of validity is more extended than that of Equation 36 (Fig. 2).

A similar study can be made for the reduced temperature coefficient of resistivity, β_g/β_f, and it can be observed that:

$$\frac{\beta_g}{\beta_f} \approx 1 + \frac{3}{8\mu}\frac{1}{1 + [C^2 - (3/8)(1-C)](1/\nu)} \quad (51)$$

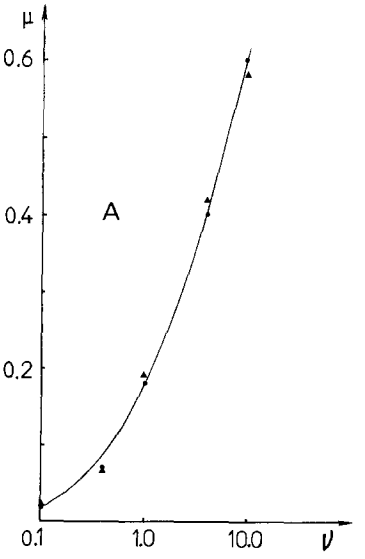

Figure 2 A is the domain where the inaccuracy of Equations 50 and 52 is less than 5% (•: polycrystalline film; ▲: columnar film).

is the most accurate expression (expressions 50 and 51 are identical).

However the validity range of Equation 51 is not larger than that of Equation 37.

3.5. Linearized reduced equations for columnar films

The same procedure as above can be implemented and leads to the following formulae:

$$\frac{\rho_{fc}}{\rho_c} \approx 1 + \frac{3}{8\mu} \frac{1}{1 + (C^2 - (3/8)C)(1/\nu)} \quad (52)$$

$$\beta_c/\beta_{fc} \approx \rho_{fc}/\rho_c \quad (53)$$

Equation 52 has a larger validity range than Equation 36 (Fig. 2). Even in this case Equation 51 does not have a larger validity range than Equation 37.

3.6. Comparison with previous calculations

Equation 50 has been previously proposed [16]; Equation 51 is very similar to the linearized expression proposed by Tellier and Tosser [4].

4. Comparison with experiments

Garcia *et al.* [30] have reported experimental data related to columnar bismuth films which exhibited quantum size effects at low temperature. At 360 K the variations in the film resistivity with thickness are in agreement with Equation 52 since a linear law is obtained by plotting ρ_{fc} versus d^{-1} (Fig. 3), except at very low thickness; extrapolating to $d^{-1} = 0$ gives the value for ρ_c: $\rho_c = 2.7 \times 10^{-4}$ Ω cm. This value differs markedly from the bulk value ($\rho_0 = 1.2 \times 10^{-4}$ Ω cm at 300 K), showing that the scattering at the grain boundary is efficient.

Since at low magnetic field the reduced Hall coefficient of thin metal films R_{Hf}/R_{H0} may be expressed as [4, 31]:

$$R_{Hf}/R_{H0} = \beta_f \rho_f / \beta_0 \rho_0 \quad (54)$$

Equations 52 and 53 give:

$$R_{Hfc}/R_{Hc} = \beta_{fc}\rho_{fc}/\beta_c\rho_c \approx 1 \quad (55)$$

in good agreement with experimental data at 360 K (see, Fig. 7 of Garcia *et al.* [30]).

At low temperature the quantum size effect appears and the theoretical equations above are not valid.

Abou-Saif *et al.* [32] have studied the structure

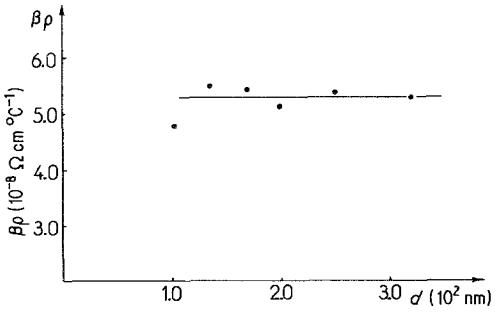

Figure 3 Variations in the resistivity of bismuth film at 360 K, ρ, versus reciprocal film thickness, d^{-1} (taken from Garcia *et al.* [30]).

of thin tin films. From the experimental data [32] related to films thicker than 100 nm, one can obtain two linear plots for the variations in ρ_{fc} and β_{fc} with the reciprocal film thickness; we then calculate $\rho_c = 12.5 \times 10^{-8}$ Ω m and $\beta_c = 4.35 \times 10^{-3}$ K^{-1}.

At lower thickness the above linearized equations are not valid (since $\nu \approx 12.7$ as calculated from ρ_c obtained by extrapolation). The values of ρ_c and β_c differ slightly from the values given by the authors [32] but they have considered the whole range of thicknesses.

The value of the product $\rho_c \times \beta_c$, 54.35×10^{-11} Ω mK^{-1}, is close to the tabulated values [33] of $\rho_0\beta_0 = 48.5 \times 10^{-11}$ Ω mK^{-1}.

Moreover the product $\beta_{fc}\rho_{fc}$ remains practically unchanged for $d > 100$ nm (Fig. 4) showing that the film has a homogeneous structure, without impurity effects.

Assuming that the electronic mean free path in the bulk material is $\lambda_0 \approx 200$ nm [32], the linear variations in ρ_{fc} with d^{-1} gives $p = 0.56$.

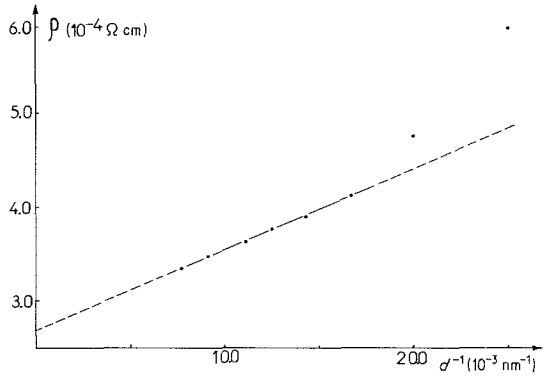

Figure 4 Variations in the product resistivity × tcr of thin tin films with film thickness, d (taken from Abou-Saif *et al.* [32]).

This value is not that much different from the value proposed by the authors [32] $p = 0.6$, using a much more sophisticated procedure. Moreover the linear plots show that the average grain size takes a constant value; this feature is in agreement with the observed [32] variations of the grain size with thickness, whose inaccuracy is approximately 28% [32]. Hence for $D_g \approx 400$ nm we calculate that $t \approx 0.85$ in good agreement with the fact that the infinitely thick film exhibits transport parameters whose values are close to those of the bulk material.

The fact that the calculated values for D_g are not constant [32] may be due to the procedure: a statistical-size distribution method, based on crystallographic data, was used [32] and it cannot be ensured that this procedure gives the average grain size for the electronic transport phenomenon.

5. Conclusion

In the framework of the statistical models describing the effects of grain boundaries and external surfaces of thin films, a set of linearized equations of large validity range can be found for ρ, β and R_{Hf} of polycrystalline and columnar films, in good agreement with experiments.

References

1. K. FUCHS, *Proc. Cambridg. Phil. Soc.* **34** (1938) 100.
2. E. H. SONDHEIMER, *Adv. Phys.* **1** (1952) 1.
3. A. F. MAYADAS and M. SHATZKES, *Phys. Rev. B* **1** (1970) 1382.
4. C. R. TELLIER and A. J. TOSSER, "Size Effects in Thin Films", Chapter 1, (Elsevier, Amsterdam, 1982).
5. C. R. PICHARD, C. R. TELLIER and A. J. TOSSER, *Thin Solid Films* **60** (1980) 157.
6. *Idem, ibid.* **62** (1979) 189.
7. C. R. TELLIER, *Electrocomp. Sci. Technol.* **5** (1979) 209.
8. C. R. TELLIER and A. J. TOSSER, *Thin Solid Films* **70** (1980) 225.
9. C. R. TELLIER, C. R. PICHARD, V. I. VATAMANYUK and A. J. TOSSER, *Int. Res. Rep. Nancy 1* **1** (1983) 1.
10. *Idem, J. Mater. Sci. Lett.* **2** (1983) 579.
11. F. WARKUSZ, *Electrocomp. Sci. Technol.* **5** (1978) 197.
12. C. R. TELLIER and A. J. TOSSER, *ibid.* **6** (1979) 37.
13. C. R. PICHARD, C. R. TELLIER and A. J. TOSSER, *ibid.* **6** (1980) 87.
14. F. WARKUSZ, *ibid.* **9** (1981) 105.
15. A. A. COTTEY, *Thin Solid Films* **1** (1967/68) 297.
16. C. R. PICHARD, C. R. TELLIER and A. J. TOSSER, *J. Mater. Sci.* **15** (1980) 2236.
17. C. R. TELLIER and A. J. TOSSER, "Size Effects in Thin Films", (Elsevier, Amsterdam, 1982) ch. 2.
18. A. J. TOSSER, V. I. VATAMANYUK, C. R. TELLIER and C. R. PICHARD, *Int. Res. Rep. Nancy 1* **2** (1983) 1.
19. C. R. TELLIER, C. R. PICHARD and A. J. TOSSER, *J. Mater. Sci. Lett.* **1** (1982) 271.
20. K. L. CHOPRA, "Thin Film Phenomena", Chapter 6, (McGraw Hill, Basingstoke and New York, 1969).
21. C. R. PICHARD, C. R. TELLIER and A. J. TOSSER, *Phys. Stat. Sol. (a)* **65** (1981) 327.
22. *Idem, J. Mater. Sci. Lett.* **1** (1982) 423.
23. *Idem, ibid.* **1** (1982) 260.
24. E. H. SONDHEIMER, *Phys. Rev.* **80** (1950) 401.
25. C. R. TELLIER, M. RABEL and A. J. TOSSER, *J. Phys. F, Met. Phys.* **11** (1978) 2537.
26. C. R. PICHARD, C. R. TELLIER and A. J. TOSSER, *Thin Solid Films* **81** (1981) 169.
27. V. I. VATAMANYUK, C. R. TELLIER, L. GUENDOUZ, C. R. PICHARD and A. J. TOSSER, *Int. Res. Rep. Nancy 1* **11** (1982) 1.
28. C. R. PICHARD, C. R. TELLIER and A. J. TOSSER, *Thin Solid Films* **69** (1980) 157.
29. *Idem, Phys. Stat. Sol. (a)* (1981) K171.
30. N. GARCIA, Y. H. KAO and M. STRONGIN, *Phys. Rev. B* **5** (1972) 2029.
31. C. R. PICHARD, A. J. TOSSER and C. R. TELLIER, *J. Mater. Sci. Lett.* **1** (1982) 260.
32. E. A. ABOU-SAIF, A. A. MOHAMED and M. G. EL-KHODARY, *Thin Solid Films* **94** (1982) 133.
33. "Handbook of Chemistry and Physics", 49th edn (The Chemical Rubber Co., Cleveland, Ohio, 1968/69).

Received 9 March
and accepted 27 March 1984